

Automated 3D Image-Based Section Loss Detection for Finite Element Model Updating

Abstract –

Accurate and rapid condition assessment of in-service infrastructure systems is critical for system-wide prioritization decisions. One major assessment consideration is structural section loss due to deterioration, for instance from corrosion. Modern 3D imaging, which generates high-resolution 3D point clouds, is capable of measuring this degradation. Despite growth in the fields of point cloud analysis, few studies have addressed the potential of using such data for creating and updating numerical finite element models of structures. This paper presents a framework for automatic and systematic 3D section loss detection in structural components, followed by a corresponding update to a finite element model. Point cloud data of a targeted structure is obtained by using recently developed Dense Structure from Motion (DSfM) algorithms. Section loss damage is then located and identified by using computer vision techniques. In order to preserve data integrity and resolve localized high fidelity details, direct 3D point cloud comparisons are applied instead of 3D surface reconstruction or curve fitting techniques that limit the accuracy of the structural analysis. An experimental case study validating the developed approach is presented, along with a discussion of potential uses for the analysis framework.

This study aims to prototype a method for fast and reliable detection, structural model updating, and tracking of deterioration in structures, for use by infrastructure managers and engineers. The proposed methodology will enable engineers to use the updated structural model to determine the reserved capacity and remaining service life of structural elements in both in-service structural systems and under severe loading conditions.

Keywords –

3D imaging; Condition assessment; Computer vision; Damage detection; Finite element model; Computational mechanics; Structural damage

1 Introduction

Existing infrastructure systems are faced with serious durability problems due to increasing service demand and natural aging. Current field inspection protocols are subjective, primarily based on visual inspection, and cannot be directly incorporated into existing numerical models of structures. Thus, there is a growing need for accurate, low cost, and consistent inspection and evaluation processes that enable more sustainable decision-making about how to repair or replace infrastructure.

3D imaging techniques are increasingly used in civil engineering applications for making 3D geometric measurements [1-3]. The fast acquisition speed, high accuracy, and portability of these modern remote-sensing tools make them an efficient and economically justifiable alternative to conventional methods. While laser scanning and photogrammetry have been used as efficient 3D measurement techniques for decades, the idea of using the acquired 3D point clouds to generate numerical structural models is relatively new. Despite the fast growth in the fields of point cloud analysis and surface reconstruction algorithms, few studies have addressed the potential of using such data for creating and updating computational models, e.g. finite element (FE) models, for structural analysis. A review of the literature [4,5] in this field not only presents a wide range of the possible applications for 3D imaging in structural engineering, but also highlights the need to develop robust methodologies for creating and updating 3D structural models. Further research is needed into the use of reconstructed 3D models of a damaged structure for updating a finite element model for the strength analysis of structural elements under in-service and severe loading conditions. The current practice of converting 3D point clouds to watertight surfaces using commercially available software in order to generate structural models may fail to preserve highly localized details of the damaged component and also limits the

scope of the anticipated structural analysis by imposing a specific type of finite element mesh.

In the current study, image-based 3D reconstruction is used to generate point cloud models of structural elements. Computer vision algorithms are then utilized to automatically locate and identify the damage in the inspected element, and finally, the structure's finite element (FE) model is updated accordingly by using an integrated methodology. The objectives of this study are 1) to evaluate the efficiency of 3D computer vision algorithms in detecting section loss in various structural element shapes, 2) to compare and evaluate the efficiency of surface reconstruction techniques in restoring the geometry and fine details of damaged regions, 3) to use the findings from Objective 1 and 2 to develop a methodology to update the structural 3D model that preserves highly localized damage on structural elements.

2 Methodology Description

The proposed methodology (Figure 1) is composed of several steps that are described in the following subsections. This methodology requires an initial solid model and point cloud data of both initial (as-built) and current conditions of the structure (i.e. undamaged and damaged) as input data. The point cloud data can be obtained by using Dense Structure from Motion (DSM) algorithms or LIDAR. In absence of as-built condition point cloud data, a 3D solid model of the initial structure (ISM in Figure 1) can be used as a basis for sampling surface points so as to generate a synthetic 3D point cloud model. In such cases, the ISM is created based on structural drawings or the building information model (BIM). The damaged and undamaged state point clouds are then compared on a point-to-point scale to detect structural deformations in the damaged component.

2.1 Data Collection

3D point cloud data of the current condition of the structure (CPC in Figure 1) is collected via a 3D laser scanner or photogrammetry (or a combination of both). Another set of point cloud data for the initial or as-built condition of the structure (IPC in Figure 1) is also generated based on the initial condition or the original structural detail drawings of the structure, respectively. The latter can be done based on the computer-aided design (CAD) model of the structure in order to generate a synthetic point cloud. The goal here is to directly compare the point cloud data of the damaged and undamaged states of the structure on a point-to-point scale and plot a deviation map. This will help to

visually represent the visible deformations in the damaged structure, detected by using 3D reconstruction and computer vision methods.

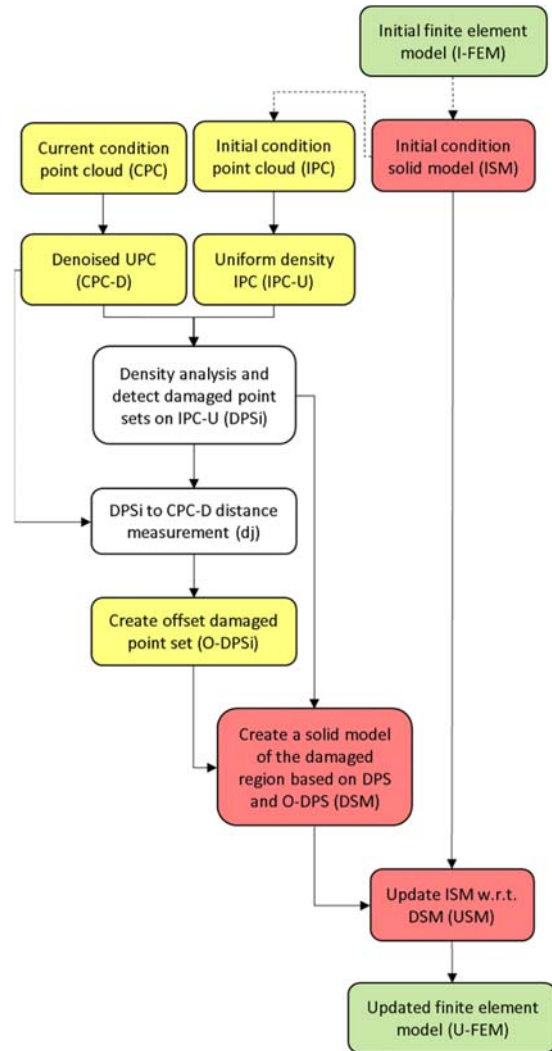


Figure 1. Flowchart of the proposed methodology

2.2 Data Preparation

The generated initial (IPC) and current (CPC) point clouds then undergo pre-processing. The goal is to create a subsampled point cloud from the initial model (IPC-U in Figure 1) in which the points are approximately spaced at an equal distance of r . In other words, the nearest neighbor point for each point in IPC-U is located at a distance equal to or slightly greater

than r . One of the most efficient ways to achieve this uniform sampling of the point cloud is by building a 3D voxel grid with the input data and taking the centroid (average point inside a voxel) of the voxel grid as a key point. The number of points in the resulting point cloud is then reduced and down-sampled uniformly. In this paper, the open source software package *CloudCompare* [6] is used for this purpose. The value for r is empirically determined and should be set by considering the desired flaw detection precision, the UPC density, and the IPC surface density. For an initial value, a radius corresponding to 24 points per square unit for the IPC model is suggested. To obtain the local point density ρ at a point \mathbf{p} , $\rho = k / r^2$, where r is the radius of the enclosing sphere of the k -nearest neighbors of \mathbf{p} , denoted by the index set N_p , given by:

$$r = \max_{i \in N_p} \|p - p_i\| \quad (1)$$

After determining the r value and generating the IPC-U model, a de-noised version of the current condition point cloud (CPC-D) is created by deleting all the points that have only one or two neighboring points within their specified r distance.

2.3 Density Analysis for Damage Detection

Intuitively, surfaces that are present in IPC-U but are not present in CPC-D correspond to deformed regions or section loss. These regions can be detected by the merging-and-isolating procedure described as follows. First, IPC-U and CPC-D are merged and, consequently, all of the points in IPC-U will find at least one neighboring point in CPC-D with a distance less than r , except for those points corresponding to the damaged regions. By isolating the points with no neighbor within their r distance, point sets corresponding to the damaged surfaces (DPS) can be found. In case of multiple scattered damaged regions, a simple segmentation procedure can be used to break DPS into i distinct separated regions (DPS _{i}) where each DPS _{i} represents a deformed surface in IPC, each composed of j points.

2.4 Cloud-to-cloud Distance Analysis for Damage Quantification

Typically, another surface is present in CPC-D for each DPS _{i} within a damaged region. An exception is a through hole for which there are two DPS _{i} on two opposite sides of IPC-U. Thus, the distance from each DPS _{i} to its corresponding surface in CPC-D can be used as a quantification measure for the extent of the damage. There are different definitions and methods to calculate the distance between two point clouds (or point sets). In

the current study, a definition based on [7] is used. For each DPS _{i} , the distance (d_j) from each point to CPC-D is then calculated. Using the method in [7], the *Hausdorff* distance for each point p in a reference cloud S is the distance to the nearest point in the other cloud S' :

$$d(p, S') = \min_{p' \in S'} \|p - p'\|_2 \quad (2)$$

The octree-based *C2C* plugin implemented in *CloudCompare* is used in this study to calculate vector d_j for each point in each DPS _{i} . In addition, the normal is estimated for each point within the point clouds using Principal Component Analysis in a local neighborhood of p as described in [8].

2.5 Reconstruct Damaged Surface

Each damaged surface in CPC-D can be estimated by offsetting the points in each DPS _{i} by each point's displacement vector d_j . This can be used to create an offset point set (O-DPS _{i}) for each DPS _{i} . The implementation of the code for this purpose was done in *Matlab*. At the end of this stage, there are two point sets for each damaged regions: a DPS _{i} corresponding to the original surface and an O-DPS _{i} corresponding to the estimated new surface in the current condition (see Figure 4h). If DPS and O-DPS are converted into their corresponding surfaces, the volume encompassed between these two surfaces will correspond to a section loss damage or surface expansion (depending on the direction of vector d_j) in the initial solid model (ISM).

2.6 Create Solid Model of the Damaged Region

The goal of this step is to use O-DPS _{i} and DPS _{i} to create a watertight volume for each of the i damaged regions. This can be done by generating a watertight surface (mesh) encompassing the volume created between each O-DPS and DPS. The created watertight surface will be then converted to a solid model. Fundamentally, surface reconstruction algorithms generate a polygonal mesh from a dense point cloud model in order to recover the original surface on which those points lie. The method developed in [9] is used in this study. The basic idea behind this method is to reconstruct triangulated surfaces that are formed by a subcomplex of Delaunay triangulation. The created mesh is then converted into a solid model (DSM) using *Autodesk Inventor* software.

2.7 Update the Initial Solid Model

Prior to updating the FE model, the last step of the

procedure involves subtraction (or addition in the case of expansion) of the solid model of the damage (DSM) from the initial solid model (ISM) via *Boolean* operators. This operation can be performed in several ways. In the current study, *Autodesk Inventor* software is used for this purpose. The final updated solid model (USM in Figure 1) can then be exported into a finite element program for further analysis.

3 Application and Results

For experimental validation, the presented methodology was tested using two specimens. The specimen geometry and material were chosen in order to easily fabricate proof-of-concept specimens and controlled damage patterns. The specimens (shown in Figure 2) included a built-up section made from medium-density fiberboard (MDF) material, and a cardboard tube. The 19 mm thick I-profile specimen represented a structural component with planar surfaces and several controlled flaws were machined using a CNC machine. The 12.7 mm thick tube specimen had an outer diameter of 127 mm and represented a structural component with a curved surface. The damage in the tube specimen included a randomly shaped hole.

In order to create accurate and highly dense 3D point cloud data for the targeted specimens before and after being damaged, an image-based 3D reconstruction technique called Hierarchical Point Cloud Generation (HPCG) [10], an adaptation of the well-known Semi-Global-Matching (SGM) algorithm [11], was employed. One of the key features of this multi-scale 3D reconstruction process is its ability to control the resolution of the point clouds at different locations, which was essential in capturing localized details of the damage in each of these specimens. Throughout this study, a Nikon D-800E (36.3 mega pixels resolution) D-SLR camera with a Nikon AF-S 50mm lens was used to capture images. All images were taken with a sensitivity (ISO) of 200 and an aperture of $f/8$.

The undamaged and damaged point clouds for the I-profile were generated using 165 and 293 images that resulted in dense 3D point clouds with 27,120,412 and 35,610,062 points, respectively. For the tube specimen test, there were 92 images and 2,405,713 points for the undamaged condition and 83 images and 11,655,611 points for the damaged condition. The average local density of points for the damaged specimen point clouds was approximately 600 and 550 points per bounding box volume (cm^3) for the I-profile and tube specimens, respectively.

3.1 I-Profile Specimen

In total, 9 defects of different shapes and sizes (DPS_i) were machined in the I-profile specimen's web. These defects are listed in Table 1 and are shown in Figure 4n. The ISM was created in *AutoCad Inventor* based on the actual dimensions of the specimen. Each defect was modeled separately following the methodology described in the previous section and the ISM was updated with one defect at a time.

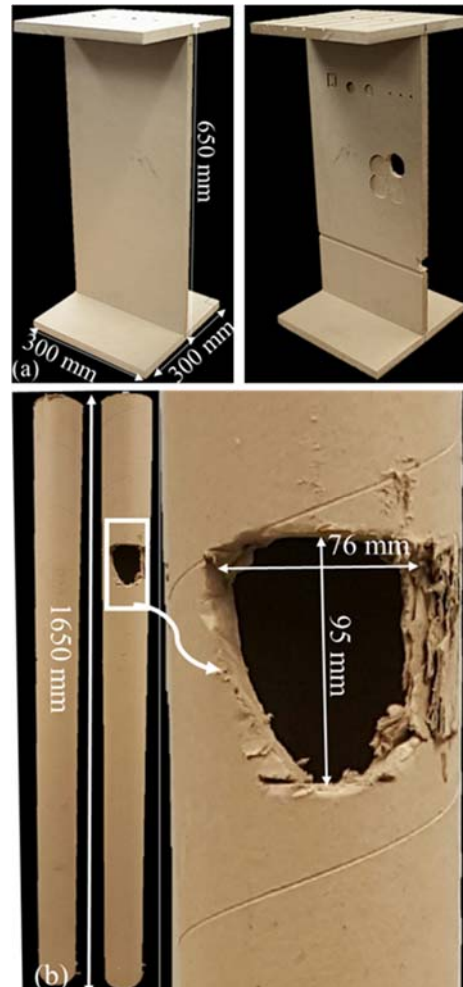


Figure 2: Undamaged and damaged specimens: (a) MDF I-profile; (b) cardboard tube

As can be seen in Table 1 and Figure 4, the first part of the methodology (i.e. the point cloud density analysis) successfully detected all of the 9 defects (DPS in Section 2.3) and the second part of the methodology (i.e. the cloud-to-cloud distance analysis) was able to provide a quantification estimate for 6 of them (O-DPS in Section 2.4). Generally, better damage extent estimations were achieved with an increase in the defect

dimensions and volume. For the defects with a minimum dimension of less than 10 mm, it was observed that the captured volumes were systematically lower than the measured values. For instance, the captured defect volume for DPS₉ (5 mm deep transverse groove) was significantly lower than the actual volume.

To further study the correlation between the captured and actual volume of the defects, the point cloud-based measurements are plotted versus the actual measurements in Figure 3. According to this figure, the correlation between the measurements improves for 10,000 mm³ and larger defects; however, the point cloud-based measurements were significantly lower than the direct measurements for smaller volumes.

Table 1: DPS_i on I-profile web

i	Defect	Depth (mm)/ Area (mm ²)	Actual Volume (mm ³)	Captured Volume (mm ³)
1	Circular hole	19/ 30.66	583	0 (detected)
2	Circular groove	4.1/ 30.66	126	0 (detected)
3	Circular groove	3.1/ 30.66	95	0 (detected)
4	Circular groove	5/ 449	2,242	607
5	Circular groove	10/ 433	4,335	1,163
6	Square groove	3.2/ 351	1,124	133
7	Connected circles	3, 5, 7, 10, 19/	98,318	88,490
8	Edge defect	19/ 288	5,472	3,214
9	Transverse groove	5.1/ 7437	37,929	6,920

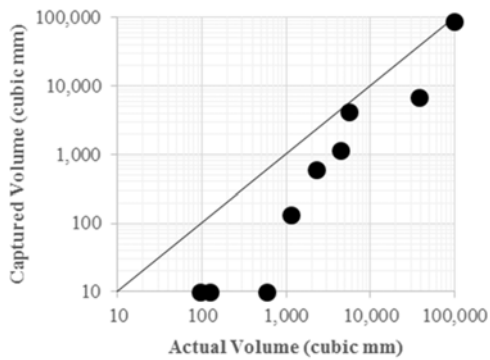


Figure 3: Captured vs. actual defect volumes

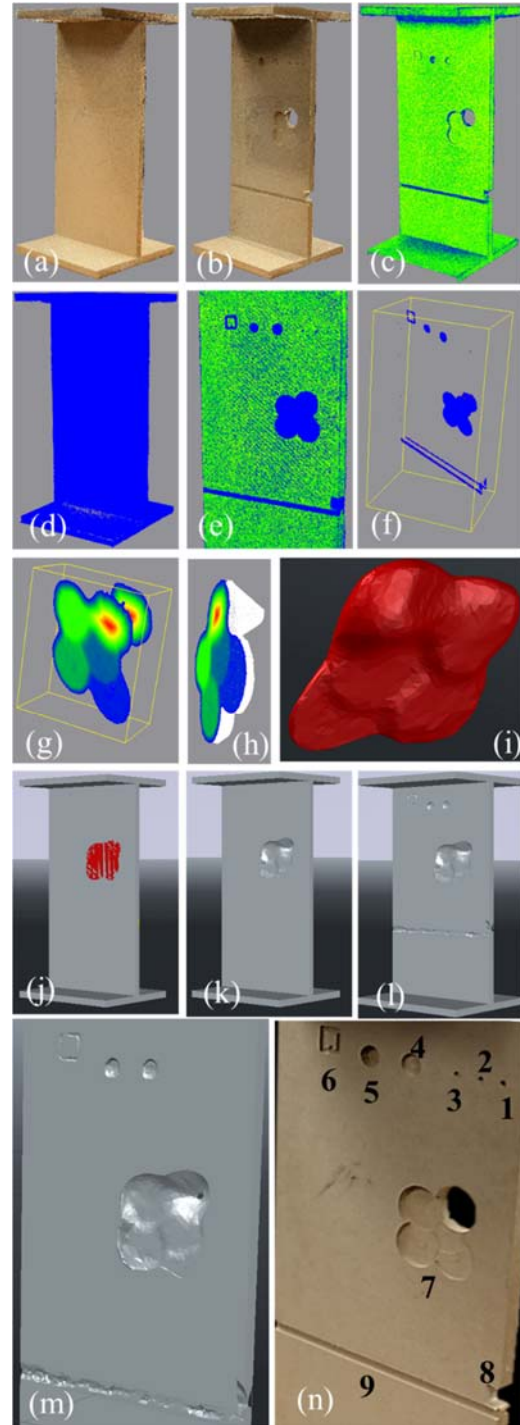


Figure 4: Updated I-section solid model: (a) IPC; (b) CPC; (c) CPC-D; (d) IPC-U; (e) merged IPC-U and CPC-D (web only); (f) detected DPS_i's; (g) calculated d_i for DPS₇; (h) O-DSP₇; (i) DSM₇; (j) ISM and DSM₇ alignment; (k) first ISM update; (l) and (m) USM; (n) DPS_i's

The employed cloud-to-cloud distance measurement technique was found to be the main reason for the systematic underestimation of the defect volumes. As can be seen in Figure 4g, the current distance definition intrinsically results in varying depth estimation (rendered as a heat map) for all of the defects. This leads to an inherently built-in defect damage threshold (here about 10 mm) that can be quantified. Consequently, the volume encompassed between the initial and offset point sets for each defect (DSP and O-DSP, respectively), will be automatically smaller than the real volume (see Figure 4h). This was particularly the case for DSP₇ where the captured volume for the through hole portion of the defect was in the form of a cone rather than a cylinder (Figure 4i and m).

3.2 Tube Specimen

To simulate a field condition assessment of a structural component, the point cloud data for the undamaged and damaged conditions of the tube specimen were collected at different times and light conditions. The undamaged data (IPC) was collected on a sunny day in November 2015 and the damaged data (CPC) was collected on a cloudy day in February 2016. This change in the condition of data collection can be seen in the RGB color information of the point clouds shown in Figure 5a and b. The defect for this specimen was a randomly shaped through hole in the pipe to simulate a burst pipe. The methodology was applied to the collected data and a summary of the results is presented in Figure 5.

Similar to the I-profile specimen, the damaged region on the specimen was detected using the density analysis described in the previous sections. As can be seen in Figure 5d, the cloud-to-cloud (C2C) distance pattern for the detected hole in the tube was similar to the pattern to the through hole in the I-profile (Figure 4g). In other words, the employed C2C distance definition provided a gradual DSM.

4 Finite Element Model Updating

Once updated, the updated solid model (USM) can be exported to a finite element program to study the structural behavior of the damaged component. In this study, the finite element (FE) program *Abaqus* was used to create the FE models of the ISM and USM.

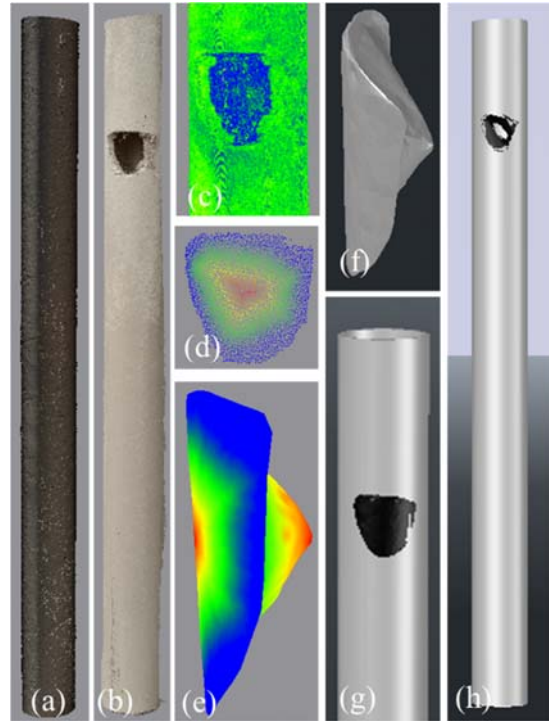


Figure 5: Updated solid model for the tube specimen: (a) IPC; (b) CPC; (c) merged IPC-U and CPC-D; (d) calculated d for DPS; (e) surface reconstruction based on DPS and O-DSP; (f) DSM; (g) ISM and DSM alignment (close up); (h) USM

The initial and updated solid models were exported in the form of an *.igs* file into *Abaqus*. After importing the geometry of the model, other model parameters including material properties, boundary conditions, and loading conditions can be defined for the FE model. Prior to the analysis, however, the model must be discretized into a finite element mesh. Typically, a finer mesh (i.e. smaller element size) is required at locations with complex geometry to capture the induced stress concentration effects. Figure 6 presents the FE mesh for the undamaged and damaged conditions of the tube specimen. As can be seen in this figure, a uniform, structured FE mesh was created for the ISM whereas a rather complex FE mesh was required for the USM to facilitate the FE analysis. In particular, a biased, fine FE meshing scheme was employed around the damaged region (through hole) as can be seen in Figure 6c.

Defining the desired type of analysis (e.g. linear or nonlinear analysis), assigning material type and properties, and defining the boundary and loading conditions will be the final steps in completing the developed point cloud-FE model updating pipeline that was presented in this study.

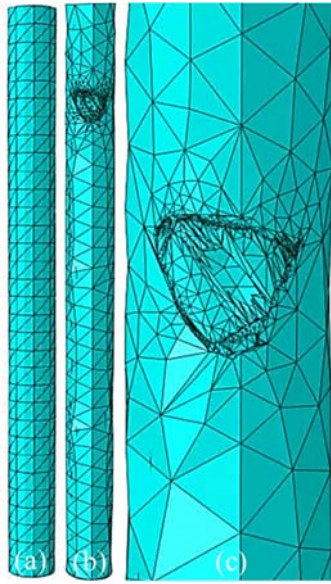


Figure 6: Finite element mesh in *Abaqus*: (a) undamaged model (I-FEM); (b) damaged model (U-FEM); (c) refined mesh in the damaged region

5 Comparison with the Current Practice

The proposed methodology has several advantages over the current practice of using commercial software for surface reconstruction (also called meshing). A number of these advantages are:

- The proposed methodology avoids applying a surface reconstruction scheme on a global scale. Instead, meshing techniques are applied at a local scale that reduces the computation time and cost significantly. For instance, the damaged I-profile specimen was reconstructed using the Screened Poisson surface reconstruction algorithm described in [12] with spatial octree depth equal to 12 and is shown in Figure 7. This model consists of more than 7 million triangles whereas the USM shown in Figure 41 had less than 15,000 triangles. The key reason for this substantial difference is that most of the triangles in the reconstructed ISM were used to model essentially flat and flawless parts of the specimen (Figure 7). The inevitably large number of triangles used in the reconstructed model makes it very difficult to perform the subsequent structural analysis. Still, the final reconstructed model will fail in preserving some basic features of ISM such as the flat surfaces and sharp edge boundaries, which due to the intrinsic definitions of these methods, will be transformed

into wavy surfaces.

- Reducing the number of triangles (decimation) and/ or smoothing the surfaces in the reconstructed model will result in the loss of important features that were already captured in the point cloud data. Using a point cloud-based approach, such as the one introduced in this paper, helps to accurately represent the localized details of the model through the model updating procedure.
- It is not easy to further update a reconstructed model based on the subsequent point cloud data obtained from future field inspections. Considering that civil structures are inspected on a regular basis, a new reconstructed model is required for each inspection. In the proposed methodology, however, the model (USM) is updated one defect at a time and, thus, damage propagation as well as new damage can be easily accommodated and tracked based on new inspection data.

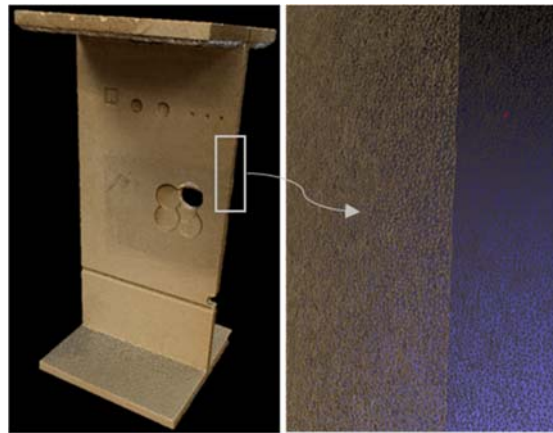


Figure 7: Reconstructed damaged I-profile with more than 35 million vertices and 7 million triangles

6 Conclusions and Future Work

In this paper, a methodology to update the finite element model of a damaged structural component based on comparative point cloud analysis was introduced. The methodology was successfully used to detect and quantify the extent of different types of damage and to then update the solid model of the member, for further finite element analysis. The proposed point cloud-based methodology has a number of advantages over the current practices, which are mainly based on localized surface reconstruction approach taken. These advantages include a significantly lower computation time and cost, the ability to preserve highly localized details of the original point cloud data, providing quantitative metrics for the

extent of damage, and the capability to further update the model based on future inspection data and for future referencing.

Based on the measurements conducted in this study, the following observations and consequent recommendations are made, with regard to FE model updating based on point cloud data:

- Good agreement was observed between the point cloud-based and direct measurements when all of the dimensions for the defect were about 10 mm or larger. The results generally improved as the magnitude of the measured dimensions increased.
- The methodology in its current form is capable of modeling section loss and corrosion expansion damage.
- The employed cloud-to-cloud distance definition caused a systematic underestimation of defect size and volume.
- A distinct distance deviation pattern was observed for the through hole defects that resulted in a cone-shaped defect rather than a cylindrical shape one.

This study was part of an on-going research program and several aspects of the presented methodology are being considered for further improvement. These aspects include:

- More advanced and robust direct cloud-to-cloud comparison techniques such as the Multiscale Model to Model Cloud Comparison (M3C2) proposed in [13].
- Using Non-Uniform Rational Basis Spline (NURBS) to create a DSM instead of using surface reconstruction methods.
- Evaluating and incorporating different registration, alignment, and de-noising algorithms to facilitate automatic updating of the FE model.
- Designing and fabricating large-scale specimens to assess the performance of the proposed methodology on large-scale specimens and possibly full-sized structural components.

This study also shows that 3D vision-based techniques offer an appropriate and practical means for structural inspection because of their portability, the relative ease of use, and the ability to archive the data for future referencing.

References

- [1] Fathi H., Dai F., Lourakis M. Automated as-built 3D reconstruction of civil infrastructure using computer vision: achievements, opportunities, and challenges, *Advanced Engineering Informatics*, 29(2):149-161, 2015.
- [2] Koch C., Paal S., Rashidi A., Zhu, Z., König M., Brilakis I. Achievements and challenges in machine vision-based inspection of large concrete structures. *Advances in Structural Engineering*, 17(3):303-318, 2015.
- [3] Koch C., Georgieva K., Kasireddy V., Akinci B., Fieguth P. A review on computer vision based defect detection and condition assessment of concrete and asphalt civil infrastructure. *Advanced Engineering Informatics*, 29(2):196-210, 2015.
- [4] Barbieri G., Biolzi L., Bocciairelli M., Fregonese L., Frigeri A. Assessing the seismic vulnerability of a historical building. *Engineering Structures* 57:523-535, 2013.
- [5] Conde-Carnero B., Riveiro B., Arias P., Caamaño J.C. Exploitation of Geometric Data provided by Laser Scanning to Create FEM Structural Models of Bridges. *Journal of Performance of Constructed Facilities*, 04015053, 2015.
- [6] Girardeau-Montaut, D. Cloud Compare: 3D point cloud and mesh processing software, open-source project. On-line: <http://www.danielgm.net/cc>, Accessed: 04/03/2016.
- [7] Girardeau-Montaut D., Roux M., Marc R., Thibault G. Change detection on points cloud data acquired with a ground laser scanner. *International Archives of Photogrammetry, Remote Sensing and Spatial Information Sciences*, 36(part 3) W19, 2005.
- [8] Hoppe H., DeRose T., Duchamp T., McDonald J., Stuetzle W. *Surface reconstruction from unorganized points*, 26(2):71-78, ACM, 1992.
- [9] Cazals F. and Giesen J. Delaunay triangulation based surface reconstruction. In *Effective computational geometry for curves and surfaces*, pages 231-276. Springer Berlin Heidelberg, 2006.
- [10] Khaloo A. and Lattanzi D. Extracting structural models through computer vision, In *Proceedings of the Structures Congress 2015*, pages 538–548, Portland, USA, 2015.
- [11] Hirschmuller H. Stereo processing by semiglobal matching and mutual information, *IEEE Transactions on Pattern Analysis and Machine Intelligence*, 30(2):328-341, 2008.
- [12] Kazhdan, M. and Hoppe H. Screened poisson surface reconstruction. *ACM Transactions on Graphics (TOG)*, 32(3), 29, 2013.
- [13] Lague D., Brodu N., Leroux J. Accurate 3D comparison of complex topography with terrestrial laser scanner: Application to the Rangitikei canyon (N-Z), *ISPRS Journal of Photogrammetry and Remote Sensing*, 82:10-26, 2013.